

Quantifying the embodied carbon of cantilevered massing typologies in architectural design

Kiley FEICKERT^{a*}, Natasha K. HIRT^a, Katrina CHAN^a, Caitlin T. MUELLER^a

^a Massachusetts Institute of Technology, Department of Architecture
77 Massachusetts Avenue, Cambridge, MA 02139, United States of America
*feickert@mit.edu

Abstract

Much of the research and discourse around embodied carbon (EC) in buildings focuses on material-scale interventions or substitutions. However, it is well documented that design decisions that leverage structural mechanics can play a significant role in reducing material consumption and the resulting EC of structural systems. Intuitively, architectural massing may have a very large impact on EC; yet, the impact is not well characterized. This research identifies building massing as a key lever in the EC outcomes of structural systems and proposes a method to quantify its impact using automated structural design and analysis. It contributes embodied carbon estimations for non-normative massing typologies common in contemporary architecture to evaluate the range in EC performance for visually similar massing proposals. It finds that cantilevered massing typologies can be materialized for no carbon penalty if efficient configurations are used, contradicting a common perception that cantilevers always come at a carbon cost. If inefficient configurations are used, they can incur a significant carbon penalty (2.4x) compared to a normative massing configuration, demonstrating that massing is a crucial lever for reducing EC in architectural design.

Keywords: Embodied carbon, Massing, Form, Conceptual design, Architectural design

1. Introduction

Reducing greenhouse gas (GHG) emissions from the construction sector is crucial for limiting global warming and creating a more environmentally responsible and equitable built future. Buildings typically require large volumes of raw materials to construct, and therefore embody large quantities of carbon. As such, embodied carbon (EC) from the building stock is responsible for 13% of annual global GHG emissions [1] (3.8 GtCO₂) [2]. However, the quantity of material required to construct each building (and the resulting emissions) depends on design decisions made by architects and engineers, which are interrelated through structural mechanics. These decisions, or levers, include structural material, typology, column spacing (span), etc., and different combinations result in significant variability in EC performance. For buildings with steel structural systems, empirical data from built projects demonstrates a 6x difference in EC intensity (~120–730 kg CO₂e/m²) [3].

Another design lever that can have a significant impact on the EC intensity of a building is the architectural massing (or form). A dominant approach to design in architecture practice involves sculpting the overall shape of a building or arranging its programmatic volumes to compose the visual and spatial experience of the building. Complex forms can be engineered and materialized due to the development of computer-aided engineering and manufacturing methods. However, depending on the design decisions made, the aforementioned design approach can uncouple a building's form from an efficient flow of forces, incurring significant material and environmental costs. Conversely, utilizing efficient combinations of design choices can require less structural material at the building scale, and expressive architecture can be achieved without significant EC penalties. Although researchers are

evaluating the impact of different design decisions on a structural system's EC intensity, the impact of architectural massing is not well characterized, presenting an opportunity addressed in this research.

2. Background and literature review

Research that quantifies the EC of structural systems to date utilizes both synthetically generated data and empirical data from real buildings. The majority of studies evaluating synthetically generated results focus on normative building configurations with extruded rectangular footprints and rectangular structural grids [4], [5], [6], [7], [8], [9], [10]. Typically, the goal of these studies is to determine a normalized EC intensity (ECI) per floor area (kg CO₂e/m²), to evaluate the EC impact of specific design decisions, such as height, column spacing, beam spacing, structural material choice, or the impact of life cycle assessment (LCA) stages, against one another. Research that estimates EC for more complex buildings focuses on structural frame design for discrete massings [11], [12].

Complex architectural forms have also been studied using empirical material take-offs from real buildings on a case-by-case basis to extract highly detailed EC data [13], [14], [15], [16], [17], [3]. These studies are mainly analyzed by the number of stories, structural material, use type (occupancy), and the scope of elements included (superstructure, foundations, envelope, interiors), but not by architectural massing. Cantilevered buildings have been studied at a limited scale for one case study building [18]. Additional research evaluates the impact of massing on a building's overall structural strategy for twisted high-rise typologies [19]. However, this study doesn't quantify EC.

Synthetically generated models have been used to explore the impact of non-normative building massing (non-rectangular footprints or massing that is variable in section) on other performance metrics such as energy use [20], [21], passive solar energy utilization [22], daylighting [23], and thermal load [24]. However, few studies explicitly evaluate the impact of massing typologies on EC, and those that do focus on height or simple massing extrusions [25]. This gap presents an opportunity to evaluate the tradeoffs between: 1) architectural massing, 2) structural typologies (both having impacts on the spatial and experiential qualities of buildings), and 3) EC performance during early-stage design.

Intuitively, massing can have a significant effect on EC because the flow of forces is dependent on the form of the building. This intuition is seen in the challenges posed by horizontal transfers and the benefits offered by continuous beams, which lower the maximum moment along their length compared to a series of simply supported beams and therefore require less material. Nevertheless, massing has not been studied as a lever for decarbonizing structural systems in a detailed manner at the building scale. This research explores the design space of cantilevered massing typologies to understand if certain forms result in better-performing EC values while remaining architecturally expressive, addressing the questions:

- How can we evaluate the ECI of complex, non-normative massing in an automated way?
- Can building massing be configured in a way that reduces ECI comparable to a normative building?
- When massing is configured inefficiently, what is the ECI impact?

3. Methodology

To evaluate the impact of massing design decisions on EC performance for complex massing, accurate structural material quantities (SMQs) are needed. This is a non-trivial technical challenge that requires automated design and dimensioning of the full structural system. Therefore, this method is designed to replicate the results of a typical structural engineering process by using an automated computational workflow that rapidly and reliably generates high-fidelity SMQs and EC data, accounting for material properties and structural mechanics. Previous research has paved the way to generate synthetic data for buildings through automated structural design and analysis [26], [27], [4], [5], [6], [7], [11], [12], [28], [29], [10]. This paper adopts a similar approach and parametrically links various massing decisions to

generative structural design and analysis models for select massing typologies. This research contributes an analysis of the ECI of these massing decisions to distinguish those that are spatially impactful, yet minimize ECI to inform early-stage massing design.

3.1. Conceptual overview

A conceptual overview of the methodology used in this paper is shown in Figure 1. The massing typologies evaluated are drawn from an analysis categorizing non-normative contemporary mid-rise buildings into typologies based on their architectural form (Section 3.2). The selected typologies are parameterized by key design decisions, such as shifting and scaling the dimensions of various floorplates (Section 3.3), and sampled to generate a synthetic dataset. Structural frames for the vertical load-resisting structural system are generated for each unique design (Section 3.4). Next, the structural floors, frame, and foundations (spread footings) are analyzed, and material quantities are extracted for each element by structural material type (Section 3.5). Lastly, SMQs are used to calculate EC to evaluate the impact of massing decisions on the global warming potential (GWP) of the parameterized design decisions (Section 3.6).

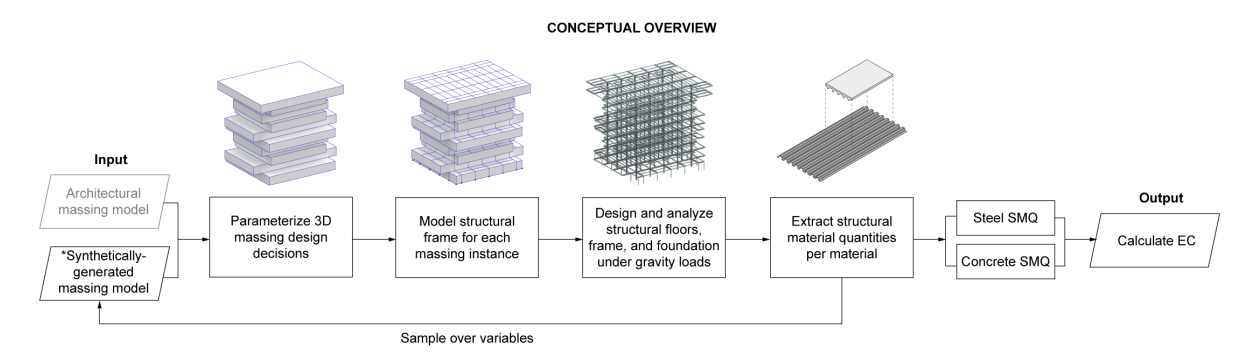


Figure 1: Conceptual overview of the methodology used to calculate structural material quantities and embodied carbon for architectural massing typologies. *Used in this paper

This research focuses on mid-rise residential and commercial projects, as the forms and structural typologies studied are most applicable to these use cases. They also have the most potential to benefit from this work. When combined, moderate-sized residential and commercial buildings are estimated to comprise the largest share of gross floor area and GWP in the U.S. [30]. Due to the massing typologies being studied, this research focuses on steel multi-story, framed buildings with non-composite steel deck and lightweight concrete (steel deck) floors. The SMQs produced using this method are expected to be lower than SMQs drawn from empirical data as the scope of this analysis does not include lateral systems (including walls, frames, and core), basements, retaining walls, or subfloors, in part because cantilevered designs primarily affect the vertical load-resisting system and are typically resolved with steel frames. However, the range in EC performance demonstrates that efficient combinations of design decisions are impactful and warrant careful consideration during early-stage design.

This paper quantifies EC in units of CO₂e, representing the environmental impact of LCA stages A1-A3, or cradle-to-gate processes, as defined by EN 15978:2011. This research focuses on Stages A1-A3 because they account for the majority of embodied emissions [16], [31], [32], and the scope aligns with the scope of most Environmental Product Declarations (EPDs) for the materials analyzed [33]. In this research, the term EC is used interchangeably with GWP, and carbon (or equivalent GHG) emissions (CO₂e).

3.2. Selecting massing typologies for evaluation

Contemporary mid-rise architecture projects are reviewed using popular architectural design publications to understand trends in building massing. Buildings that have non-normative massing are

categorized based on their visual characteristics. "Stacked boxes" are selected due to their prevalence and the structural complexity introduced by cantilevers. Because of the non-direct load path, this massing typology has the potential to introduce significant material and environmental costs. Stacking boxes has become such a popular massing typology that prominent architecture publications such as Dezeen and Architizer have dedicated keyword tags and blog posts to the topic [34], [35]. In fact, Dezeen features 108 projects dating back to 2007, tagged with the keyword *irregularly stacked boxes* [34]. For the purpose of this research, the typology stacked boxes is used to describe buildings with rectangular floorplates that scale and/or shift in the x- and y-directions relative to adjacent floors. Scaling and shifting are defined as a variable for each floor in both the x- and y-directions (Section 3.3).

Due to the high dimensionality of the design space for ten-story stacked boxes (20–40 variables), a building with a single floor that is cantilevered in one direction and two directions (1 variable) is also studied to evaluate the impact of massing on ECI. These massing typologies are shown in Figure 2.

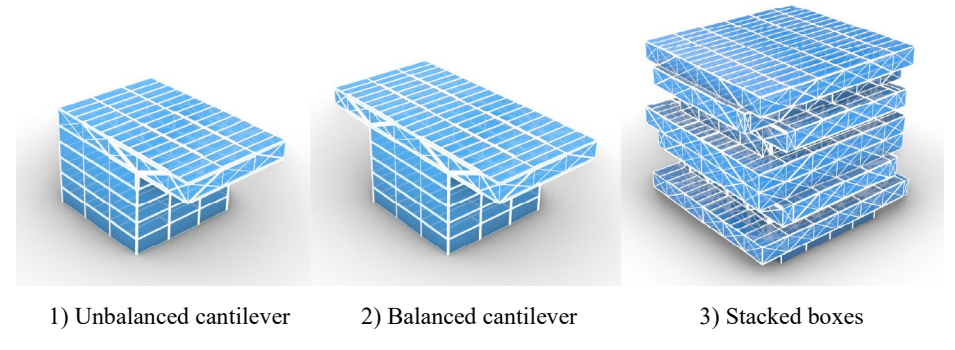


Figure 2: Select massing typologies in contemporary architecture studied in this research

3.3. Massing parameterization

Massing typologies with various overhang dimensions and configurations are studied to understand the implications of massing design decisions on their required EC. First, to isolate the effect of a single overhang, a cantilever is parameterized to extend in one dimension (in increments of 0.6 m) for: 1) a truss with an unbalanced cantilever (Figure 2.1), 2) a truss with a balanced cantilever (Figure 2.2), and 3) a frame with an unbalanced cantilever (not shown). All designs have six stories, a 27 m x 27 m footprint, 9 m x 9 m primary spans, and 3 m secondary spans. Each design is compared to a baseline design with normative massing (footprint extruded vertically, all beams pinned).

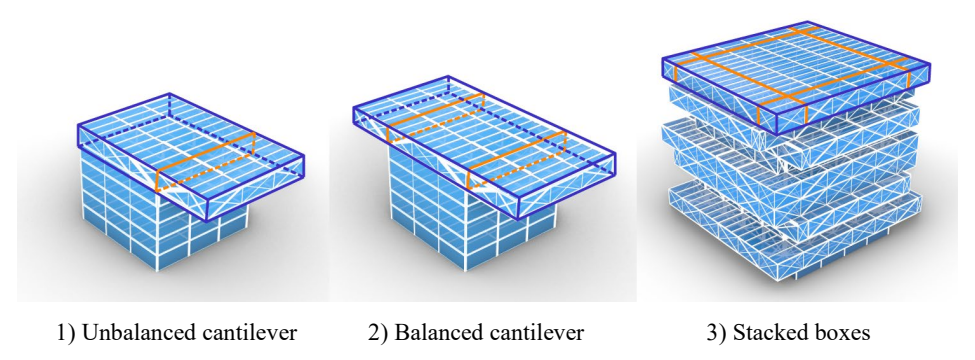


Figure 3: Belt trusses are located around the perimeter (purple), and core trusses are located along the core extending out to the façade (orange) on the top level for unbalanced and balanced cantilevers, and on all levels for stacked boxes.

To demonstrate the bounds of the best- and worst-performing configurations associated with different heuristics, two structural framing typologies are evaluated for all massing typologies:

1. Frame: No trusses, moment-connected primary and secondary beams, and

2. Truss: Core trusses, belt trusses, moment-connected primary beams, and pinned secondary beams (Figure 3).

Second, a synthetic dataset is generated to study the impact of massing design levers on the ECI of the stacked boxes typology (Figure 2.3). A normative building is modeled to serve as a baseline for comparison using boundary representations (BREPs), with 10 floors, 4 m floor-to-floor (F.T.F.) height, a 36 m x 36 m footprint, 9 m x 9 m primary spans, 3 m secondary spans, and pinned connections. Next, four design levers are parameterized in Grasshopper3D [36] for each floor level: 1) scale in the x-direction, 2) scale in the y-direction, 3) shift in the x-direction, and 4) shift in the y-direction (Figure 4). The average cantilever depth (m) and the average back-span (m) are calculated to provide a concise means of comparison. Scaling in the x- and y-directions is constrained to +/- the primary bay dimension, or 9 m in this analysis, resulting in floorplate dimensions ranging between 27 m and 46 m square. A much larger cantilever is possible in practice, but requires bespoke structural design and analysis. By limiting the bounds of shifting and scaling, designs that would require custom solutions were removed from the results. Shifting in the x- and y-directions is constrained to 4.5 m. Once parameterized, Design Space Exploration [37] is used to sample 2,000 designs across the variables outlined.

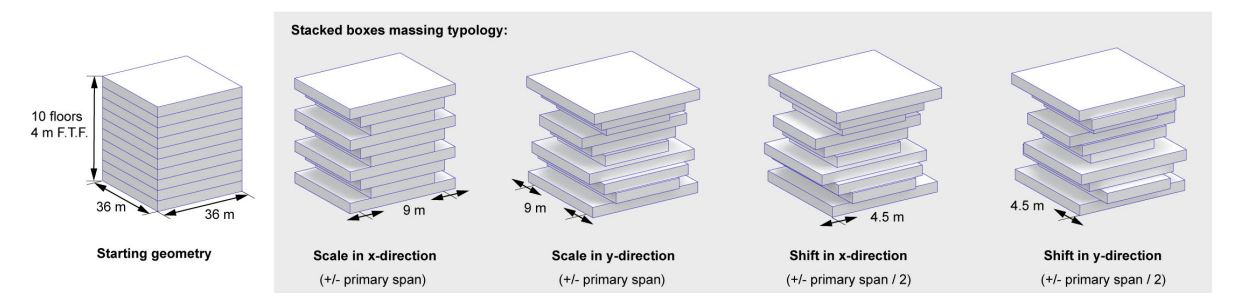


Figure 4: Select design decisions are parameterized for each massing typology to generate a synthetic dataset

3.4. Auto-framing: Modeling the structural frame for each massing instance

The parameterized massing models are the starting point for generating a parameterized 3D framing model. First, the rectangular region where all BREPs overlap in plan (referred to as the core in this analysis) is determined and projected to the construction plane (c-plane) (see Figure 5). The column grid is initialized by dividing the x- and y-dimensions of the core equally by a multiple close to, but not exceeding, the primary bay size (9 m in this analysis). The column grid is extrapolated beyond the core and vertically projected to the ceiling of each massing BREP (a surface). Points that do not immediately fall on the surface are either discarded at that level or snapped to the perimeter.

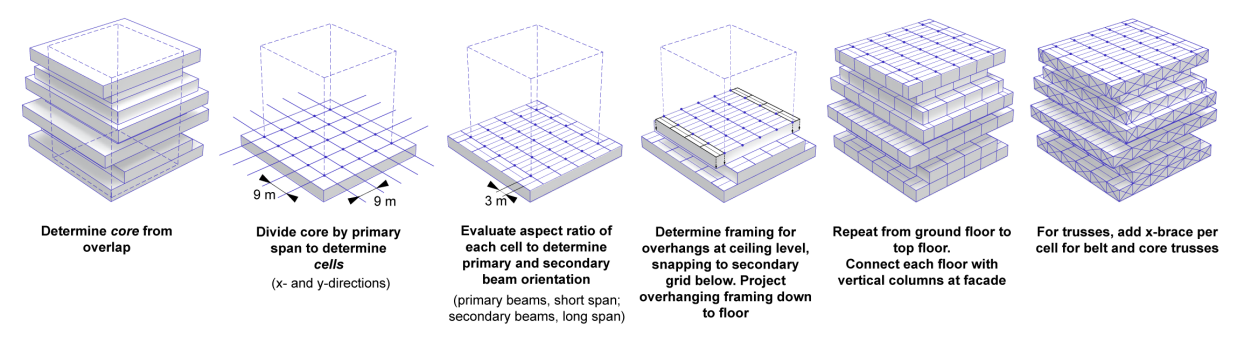


Figure 5: Automatic structural frame design for stacked boxes massing typology

The column grid is connected by primary beams to form rectangular cells, which are spanned by secondary beams. The secondary beam position is determined by measuring the x- and y-dimensions of each cell, and subdividing the short direction by a multiple close to, but not exceeding, the maximum secondary span (3 m in this analysis). These divisions determine the start- and end-points of the

secondary beams. This heuristic constrains secondary beams to span the long direction of the cell. If the short and long dimensions are similar, the side oriented along the x-axis is taken as the long dimension.

Secondary beams are generated level-by-level from the bottom up to enforce some regularity in the framing of irregular geometries. Before secondary beams are generated for a new level, its column grid is modified to snap to the nodes (secondary and column) of the level below unless the protrusion is greater than half the allowable maximum span of the secondary system. This guarantees that over- and under-hangs are vertically aligned with the level below without constraining new overhangs. Columns are generated by extruding the snapped grid points vertically until they meet the lower level.

Once framing is performed for the ceiling of each BREP, its floor is considered. Due to the overlapping quality of the massing, the combined required framing plan of the ceiling and floor may protrude beyond the original floor framing (the ceiling of the BREP below) to form a larger rectangular or cruciform floor plate. New cells are generated using an iterative flood-fill method, whereby as long as new cells were generated in the last loop, the algorithm continues evaluating whether the ceiling of the BREP contains framing cells that are adjacent to but are not found in the floor, and copies them down. Then, secondary beams are generated on a cell-by-cell basis using the heuristics described above.

Vertical framing (columns) is included in the cantilevered regions where the primary lines meet the vertical face of the new BREP, spanning the height of one floor. Although the façade is not included in this analysis, these vertical members ensure that sequential floors do not deflect unevenly. For the truss structural framing typology, cross-bracing is used, with one brace per cell. The curves and supports generated using this method are then used for structural design and analysis.

3.5. Structural design and analysis

Once structural frame models are generated, vertical load-resisting structural systems (floors, beams, columns, and foundations) are designed in detail using bottom-up, physics-based calculations following the method described in previous work by the authors [10]. An overview of this method is shown in Figure 6. Each structural system is designed to support office program (Occupancy Group B), meet the 2021 International Building Code (IBC) [39] and achieve a 2-hr minimum fire-resistance rating. An overview of the method is shown in Figure 6, and structural design loads are outlined in Table 1.

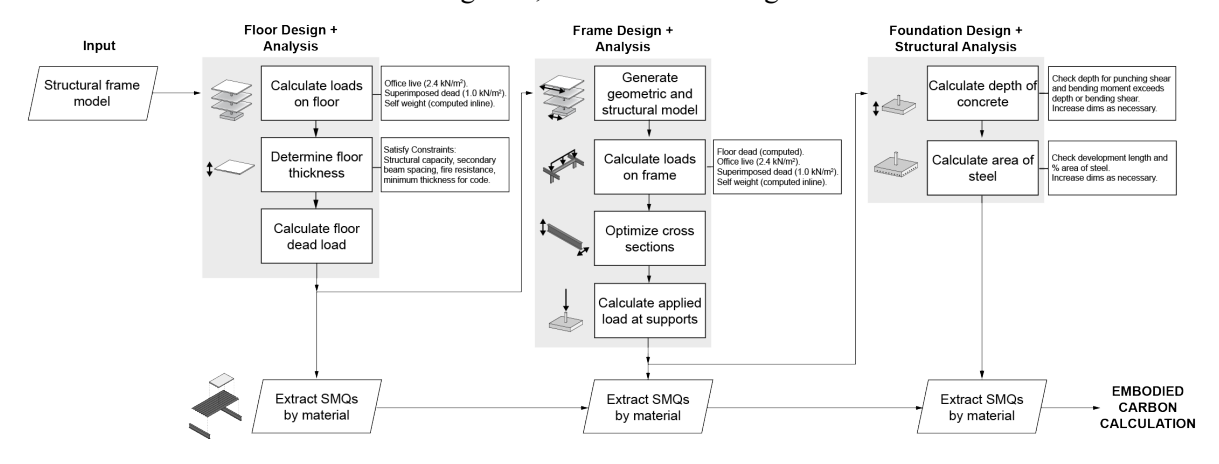


Figure 6: Methodology for structural system design and analysis (adapted from previous work by the authors [10], [38])

Table 1: Design loads for structural design and analysis (*2021 IBC [39])

Uniform live load* (kN/m²)	2.4
Superimposed dead load (kN/m²)	1
Self weight	Computed inline

3.5.1. Floor design

One-way spanning steel deck floors are designed using technical documentation from Vulcraft [40]. All floors and roofs are designed with floor loading as a conservative estimate and to allow for occupiable external terraces. To achieve the 2-hour fire-resistance rating, a 3VLI-36 composite deck is designed with a 22-gauge deck (depth of 7.62 cm), and a total slab depth of 15.88 cm; A typical build-up in North American construction (see Table 2). The secondary beam spacing is constrained to a maximum of 3 m.

Table 2: Calculated floor dead load for structural frame design

Floor System	Deck depth (cm)	Total slab depth	Dead load (kN/m²)
	(CIII)	(cm)	(KIN/III)
Steel deck with LW structural concrete topping	7.62	15.88	2.17

3.5.2. Frame and foundation design

An automated structural design and analysis framework is used to accurately size and extract material quantities for the structural frame and foundations using Finite Element Analysis. All frames are constrained by a utilization limit of 0.75 and a maximum displacement of span/120 (7.5 cm). Massing configurations that are unable to meet the maximum displacement limit (7.5 cm) or require custom cross-sections are culled from the results.

Spread footings are engineered to distribute column loads axially to sandy soil (soil bearing capacity, $q = 97kN/m^2$), following the procedures outlined in *Design of Foundation Systems* [41]. Concrete depth and steel area are calculated to meet Indian Standard 456-2000: Plain and Reinforced Concrete Code of Practice [42] due to the ability to compare typical spread footings against more materially efficient typologies in future work. This code is comparable, but more conservative than ACI 318-19 [43] in some regards [44].

Throughout the design of the structural system, SMQs are tracked and extracted for the floors (steel deck, lightweight concrete, steel mesh), frame (steel section), and foundations (steel reinforcement, concrete). These SMQs are then used to calculate embodied carbon. Embodied carbon is also calculated using the method described in detail in previous work [10].

3.6. Embodied carbon calculation

Embodied carbon coefficients (ECCs) are calculated to give comparable units across materials using the baseline GWPs in CLF's North American Material Baseline (NAB) report (2023) [33] (unless otherwise noted). ECCs represent the amount of CO₂e emitted (in kg CO₂e/kg of material) during LCA Stages A1-A3 (EN 15978:2001). For steel mesh, the values for steel rebar are used, as there is no CLF baseline GWP due to a lack of adequately representative data. The material properties and ECCs used to calculate EC are shown in Table 3.

Table 3: Material properties for structural design and embodied carbon calculations. North American baseline (NAB) ECCs are calculated to give comparable units across materials; *Steel rebar values are used.

Material	Strength (Grade) (Mpa)	Density (kg/m ³)	NAB ECC (kg CO2e/kg)
Concrete (normal)	34.5	2400	0.15
Concrete (lightweight, structural)	34.5	1800	0.33
Steel section (hot-rolled, fabricated)	415 (A572Grade50)	7850	1.22
Steel reinforcement and *steel mesh	415	7850	0.85
Steel deck (hot dip galvanized)	415	7850	2.32

Finally, embodied carbon is calculated using Eq. 1. The volume, V, of each material is multiplied by its density, ρ , and embodied carbon coefficient, ECC, to determine the total kg CO_2e for each of the building designs.

$$Embodied\ carbon = V * \rho * ECC \tag{1}$$

The total EC of each building is normalized by floor area for comparison and reported as embodied carbon intensity (ECI) in Section 4.

4. Results

4.1. Embodied carbon intensity of buildings with unbalanced and balanced cantilevered massing in one direction

Buildings with cantilevers in one direction can achieve a similar ECI as a baseline building with normative massing, up to a point (see Figure 7). For the three structural typologies studied (frame—unbalanced, truss—unbalanced, and truss—balanced) (Section 3.3), overhangs come at negligible carbon penalty up to 6 m (1:0.22 backspan to cantilever ratio), contradicting a common conception that cantilevers always come at a carbon cost. This is due to the ability to balance the moment between the cantilever and the backspan, reducing the peak moment. The overhangs also provide additional architectural and experiential benefits that are not quantified in this research, such as occupiable outdoor terraces and additional floor area for the same footprint at ground level. Beyond 6 m, the overhang increases the normalized EC compared to the baseline design (174 kg CO₂e/m²).

For smaller overhangs (0–11.4 m), the truss designs are slightly more carbon-intensive than the frame designs due to the added weight of the additional structural members. However, as the overhang dimension increases beyond 11.4 m (1:0.44 backspan to cantilever ratio), the truss becomes much more material efficient than the frame (249 kg CO₂e/m² compared to 401 kg CO₂e/m², respectively, for a 12.6 m overhang). The steep increase in the frame's material consumption is attributed to the cross-sectional area necessary to achieve the stiffness required for such a span without additional bracing. The frame also faces a significant manufacturability challenge compared to the truss designs, as it depends exclusively on moment connections for stiffness, which are time-consuming and expensive.

The balanced truss design incurs an EC penalty compared to the unbalanced truss design for overhangs greater than 6 m (ranging from 211–304 kg $CO_{2}e/m^{2}$ (balanced) compared to 197–272 kg $CO_{2}e/m^{2}$ (unbalanced)), as the backspan dimension is not increased with the added load. However, the balanced design has the potential to provide two times the outdoor occupiable area of the unbalanced designs. Taking 10.8 m overhang as an example, the roof area of the balanced design can be increased by 80% (583.2 m²) for a 40% increase in ECI (243 kg $CO_{2}e/m^{2}$) over the baseline design compared to a 40% increase in roof area (291.6 m²) for a 37% increase in ECI (238 kg $CO_{2}e/m^{2}$) for the unbalanced design. The range in carbon intensity across the spans and structural typologies studied highlights the role that massing plays in a building's EC performance and the necessity to evaluate these tradeoffs during early-stage design.

These findings demonstrate that intelligently calibrated cantilevers can be achieved without incurring carbon penalties, proving there is room for architectural expression in low-carbon design. However, in the worst cases, non-normative massing may double the EC of a building structure, confirming that massing can play a significant role in ECI and requires careful consideration during early-stage design.

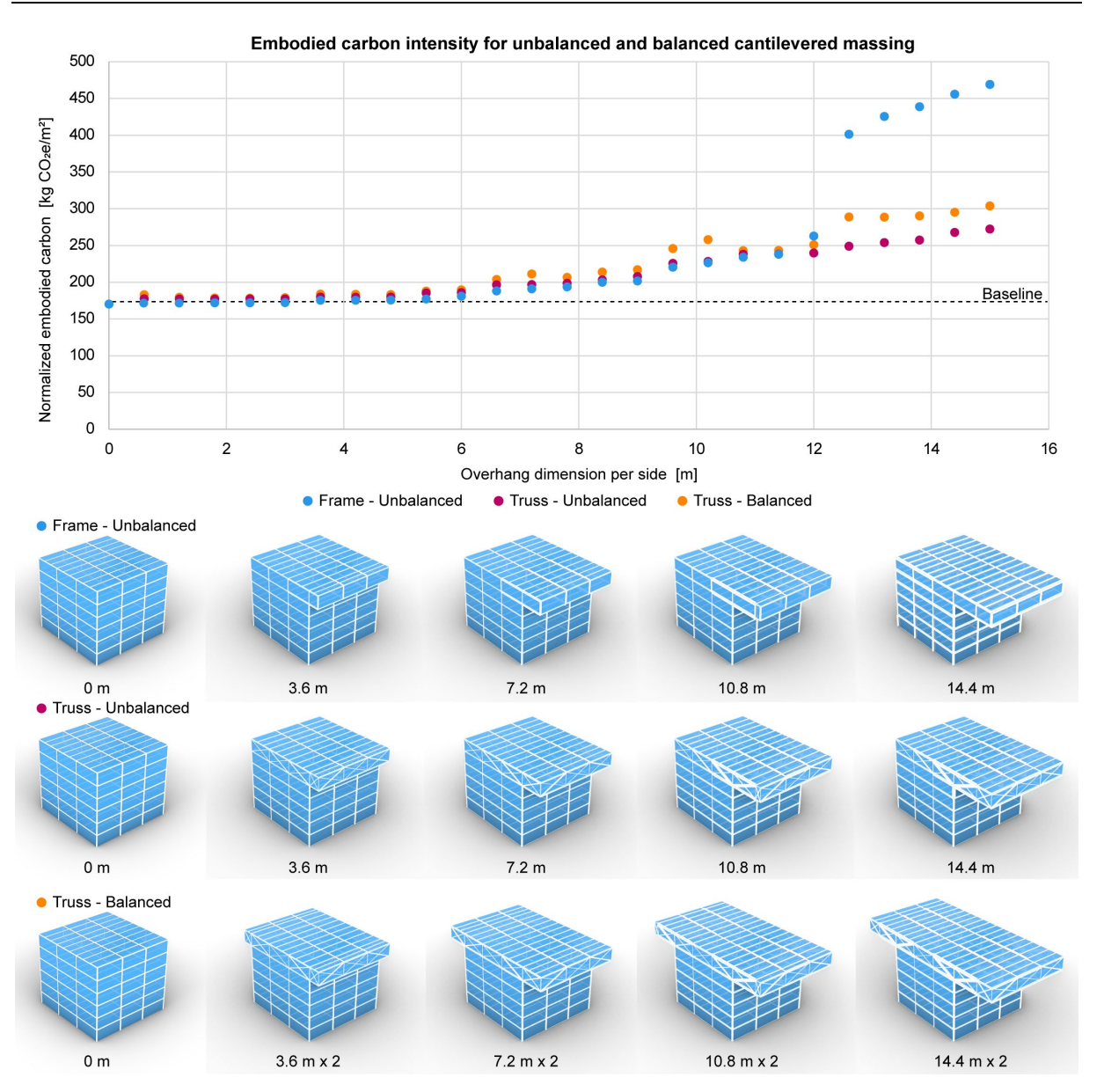


Figure 7: Unbalanced and balanced cantilever massing typologies can be materialized for a negligible EC penalty while achieving additional architectural and experiential benefits up to a point. Beyond that point, they come at a significant EC price

4.2. Embodied carbon intensity of buildings with balanced stacked boxes massing

Across the average overhangs studied, and within the same average overhang dimension, building designs with balanced stacked boxes massing demonstrate a significant range in EC performance (192–373 kg CO₂e/m² and 221–362 kg CO₂e/m², respectively) compared to the baseline design (188 kg CO₂e/m²) (Figure 8). Although the ECI range for frame and truss structural typologies is similar, only results from the truss typologies are highlighted in Sections 4.2 and 4.3 due to the anticipated ease of construction compared to a fully moment-connected frame of the same configuration. The range in ECI for the same average overhang dimension demonstrates that some designs can be very carbon efficient, while others can significantly increase the carbon intensity for similar architectural effects. For example, for a 7 m average cantilever depth, stacked box designs range from 221 kg CO₂e/m² (Design 366) to 362 kg CO₂e/m² (Design 69), representing an 18–93% increase in ECI, respectively, over the baseline.

Interestingly, the design space of the best-performing designs across the spans studied is relatively flat, with a slight trend upward, demonstrating that some building designs can have larger overhangs while only modestly increasing the ECI. For example, the best-performing designs with a 3 m average overhang incur a 5% increase in ECI over the baseline (197 kg CO₂e/m²), and designs with a 6 m average overhang incur an 11% increase (209 kg CO₂e/m²). If these designs utilize a lighter floor system, there is the potential for these configurations to achieve performance similar to that of the base case. However, this requires further study.

The flatness of the design space and the range in ECI for the same average overhang dimension confirm the finding from Section 4.1. Non-normative massing typologies can be achieved for a small carbon penalty if efficient configurations are used. If inefficient configurations are used, they can incur a significant carbon penalty over a normative massing configuration.

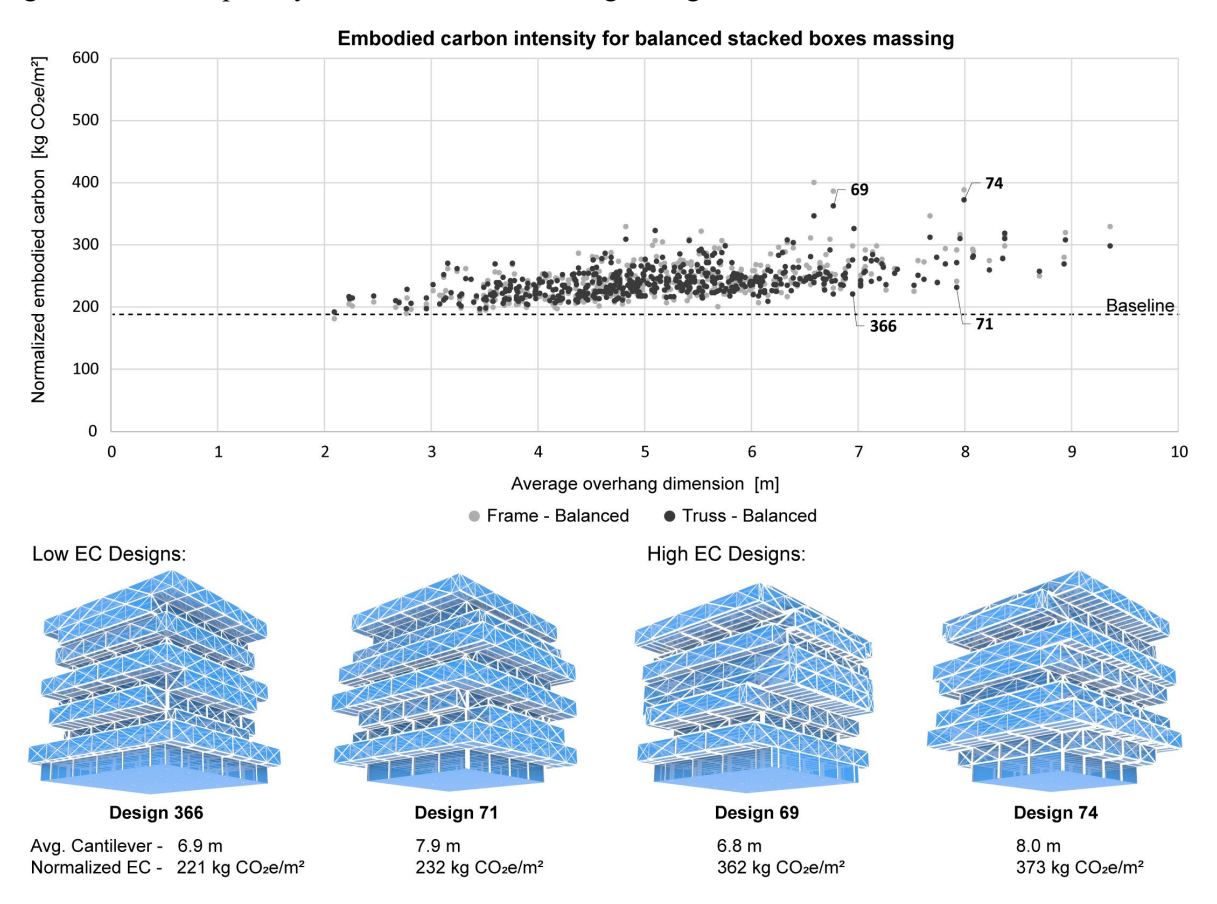


Figure 8: The embodied carbon intensity for balanced stacked boxes massing demonstrates a flat design space for the best-performing designs and a 2x difference in performance for the worst-performing designs

4.3. Embodied carbon intensity of buildings with unbalanced stacked boxes massing

When unbalanced stacked boxes are included by introducing shifts, the results show an even larger range in EC performance across designs, as demonstrated by the results in Figure 9.

In general, when floorplates are shifted, ECI increases. The same flatness of the best-performing designs from Section 4.2 is seen, demonstrating that efficient combinations are still possible, but at a slightly higher carbon price. For example, the best-performing unbalanced design with a 3 m average overhang incurs a 14% carbon penalty (215 kg CO₂e/m²) over the baseline design, compared to 5% for the balanced design. At 6 m, this difference is more pronounced with the unbalanced design incurring a 21% penalty (228 kg CO₂e/m²), compared to an 11% penalty for the balanced design. The number of

designs that did not meet the deflection limit and required custom cross-sections also increased significantly from the balanced configurations (from 18 to 168, respectively).

A noticeable shift occurs in the range of EC performance for all average overhang dimensions as well. Whereas the most material-intensive design with 7 m balanced overhangs nearly doubled the ECI of the baseline design (Design 69, 362 kg CO₂e/m², 96% increase), the most material-intensive design with 5.5 m unbalanced overhangs increases ECI by 140% (Design 393, 449 kg CO₂e/m²). However, a different massing configuration achieves a larger average overhang dimension, 6.2 m, with a significantly lower ECI, 228 kg CO₂e/m² (Design 59, 21% increase). This reinforces the finding that massing design decisions can have a significant impact on ECI and, therefore, warrant careful consideration.

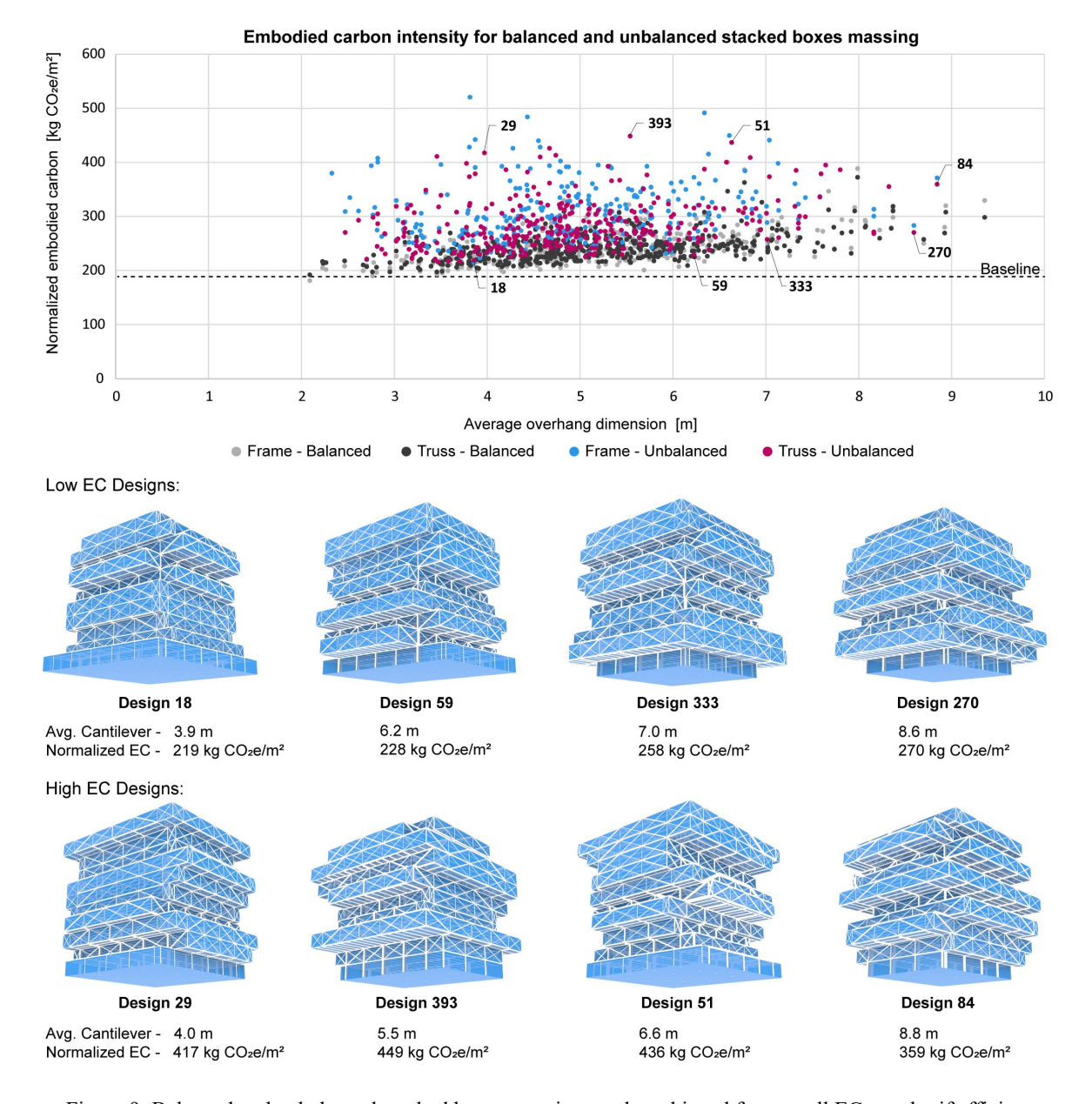


Figure 9: Balanced and unbalanced stacked boxes massing can be achieved for a small EC penalty if efficient configurations are used. If inefficient configurations are used, they can incur a significant carbon penalty over normative massing.

Although the high dimensionality of the design space makes it challenging to attribute performance to a specific variable, Figure 10 reveals that designs with a smaller average backspan typically result in higher ECI compared to designs with a larger average backspan, confirming first principles knowledge about moment balancing.

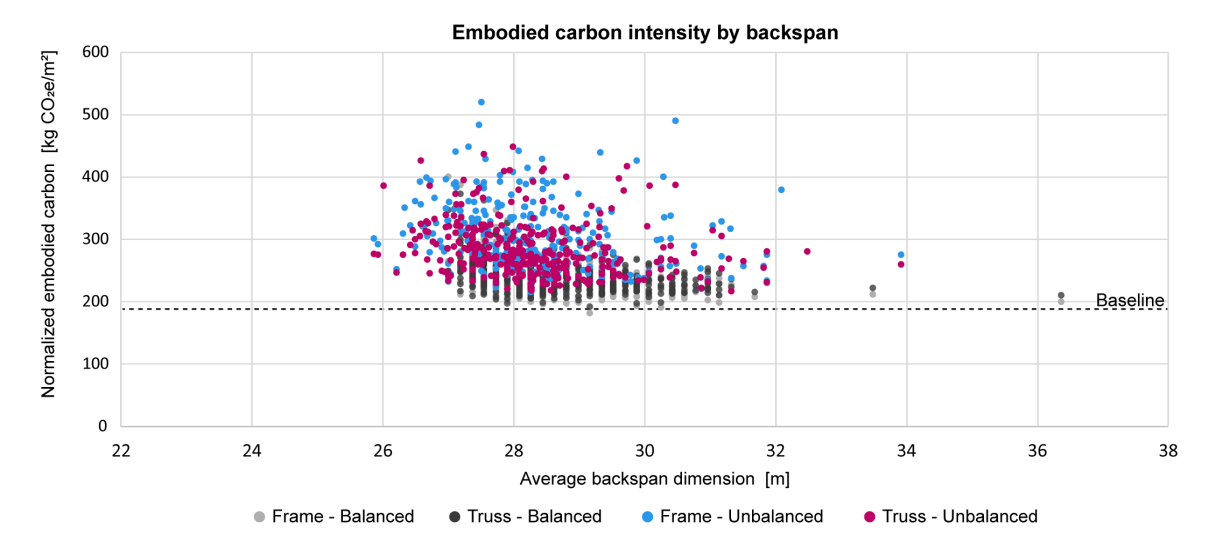


Figure 10: Embodied carbon intensity increases when the backspan decreases for the stacked boxes massing typology

5. Discussion and conclusions

This research identifies building massing as a key lever in the EC performance of structural systems and proposes a method to quantify its impact. The findings demonstrate that, surprisingly, there are ways to achieve similar EC performance in cantilevered massing typologies compared to normative massing. At the same time, cantilevered massing can result in a significant range in EC performance (188–449 kg CO²e/m²). This suggests that architects and engineers should intentionally consider how building massing impacts EC during early-stage design, and that a data-informed approach can help minimize material consumption while achieving spatially interesting forms. By considering buildings holistically, rather than focusing exclusively on material- or component-scale interventions, architects, engineers, and policymakers can leverage structural mechanics and the flow of forces to their advantage, reducing embodied carbon without compromising on design.

6. Acknowledgements

Funding for this research was generously provided by the Homer A. Burnell (1928) Presidential Fellowship, administered by the Office of Graduate Education, Massachusetts Institute of Technology; the Martin Family Society of Fellows for Sustainability, administered by the MIT Environmental Solutions Initiative, Massachusetts Institute of Technology.

7. References

- [1] International Energy Agency, "IEA, Global CO2 emissions from buildings, including embodied emissions from new construction." Paris, 2022. Accessed: Apr. 01, 2024. [Online]. Available: https://www.iea.org/data-and-statistics/charts/global-co2-emissions-from-buildings-including-embodied-emissions-from-new-construction-2022
- [2] International Energy Agency, "Perspectives for the Clean Energy Transition: The critical role of buildings," 2019.
- [3] B. Benke, A. Jensen, M. Chafart, K. Simonen, and M. Lewis, "Embodied Carbon Benchmark Report: Embodied Carbon Budgets and Analysis of 292 Buildings in the US and Canada," Carbon Leadership Forum, Apr. 2025. [Online]. Available: https://carbonleadershipforum.org/the-embodied-carbon-benchmark-report/
- [4] P. Foraboschi, M. Mercanzin, and D. Trabucco, "Sustainable structural design of tall buildings based on embodied energy," *Energy and Buildings*, vol. 68, pp. 254–269, Jan. 2014, doi: 10.1016/j.enbuild.2013.09.003.
- [5] B. D'Amico and F. Pomponi, "On mass quantities of gravity frames in building structures," *Journal of Building Engineering*, vol. 31, p. 101426, Sep. 2020, doi: 10.1016/j.jobe.2020.101426.
- [6] J. Hart, B. D'Amico, and F. Pomponi, "Whole-life embodied carbon in multistory buildings: Steel, concrete and timber structures," *Journal of Industrial Ecology*, vol. 25, no. 2: Material Efficiency for Climate Change Mitigation, pp. 249–537, 2021.
- [7] H. L. Gauch, W. Hawkins, T. Ibell, J. M. Allwood, and C. F. Dunant, "Carbon vs. cost option mapping: A tool for improving early-stage design decisions," *Automation in Construction*, vol. 136, p. 104178, Apr. 2022, doi: 10.1016/j.autcon.2022.104178.
- [8] L. Sory, "Physics-based Estimates of Structural Material Quantities for Urban-level Embodied Carbon Assessment in Buildings," Massachusetts Institute of Technology, 2023.
- [9] Y. (Lucy) Lyu, "Early Stage Embodied and Operational Analysis for Guiding Sustainable Architectural Design Decisions," Massachusetts Institute of Technology, 2023.
- [10]K. Feickert and C. T. Mueller, "Policy and design levers for minimizing embodied carbon in United States buildings: A quantitative comparison of current and proposed strategies," *Building and Environment*, p. 112485, Dec. 2024, doi: 10.1016/j.buildenv.2024.112485.
- [11] R. E. Weber, C. Mueller, and C. Reinhart, "Generative Structural Design for Embodied Carbon Estimation," in *Proceedings of the IASS Annual Symposium 2020-21 and the 7th International Conference on Spatial Structures*, Aug. 2021, p. 12.
- [12] N. Hirt, "Generative Structural Design: An Algorithmic Approach to Synthesizing and Optimizing Steel Lateral Systems," Massachusetts Institute of Technology, 2023. [Online]. Available: https://dspace.mit.edu/handle/1721.1/151830
- [13] C. De Wolf, F. Yang, D. Cox, A. Charlson, A. Seif Hattan, and J. Ochsendorf, "Material quantities and embodied carbon dioxide in structures," *Engineering Sustainability*, vol. 169, no. 4, p. 12, Aug. 2016.
- [14] K. Simonen, B. Rodriguez, S. Barrera, M. Huang, E. McDade, and L. Strain, "Embodied Carbon Benchmark Study: LCA for Low Carbon Construction," The University of Washington, Part One Version 1.0, 2017. [Online]. Available: http://hdl.handle.net/1773/38017
- [15] A. M. Moncaster, F. N. Rasmussen, T. Malmqvist, A. Houlihan Wiberg, and H. Birgisdottir, "Widening understanding of low embodied impact buildings: Results and recommendations from 80 multi-national quantitative and qualitative case studies," *Journal of Cleaner Production*, vol. 235, pp. 378–393, Oct. 2019, doi: 10.1016/j.jclepro.2019.06.233.
- [16] Röck, Martin *et al.*, "Towards embodied carbon benchmarks for buildings in Europe #2 Setting the baseline: A bottom-up approach," Zenodo, 2022. doi: 10.5281/ZENODO.5895051.
- [17]D. Fang, M. Chafart, M. Torres, and J. M. Broyles, "SE 2050 Commitment Program: 2023 Data Analysis and Findings Report," American Society of Civil Engineers, Mar. 2025. [Online]. Available: https://ascelibrary.org/doi/book/10.1061/9780784485927

- [18] J. Helal, D. Trabucco, D. Ruggiero, P. Miglietta, and G. Perrucci, "Embodied Carbon Premium for Cantilevers," *Buildings*, vol. 14, no. 4, p. 871, Mar. 2024, doi: 10.3390/buildings14040871.
- [19]Y. Erkoç and N. Torunbalcı, "Design of Twisted-Form Buildings: Correlation between Architecture and Structure," *Journal of Architectural Engineering*, 2024, doi: 10.1061/JAEIED.AEENG-1729.
- [20]T. Dogan, C. Reinhart, and P. Michalatos, "Automated multi-zone building energy model generation for schematic design and urban massing studies".
- [21]D. Ndiaye, "The impact of building massing on net-zero achievability for office buildings," *Build. Simul.*, vol. 11, no. 3, pp. 435–438, Jun. 2018, doi: 10.1007/s12273-017-0417-5.
- [22]L. Wang, K. W. Chen, P. Janssen, and G. Ji, "ALGORITHMIC GENERATION OF ARCHITECTURAL MASSING MODELS FOR BUILDING DESIGN OPTIMISATION," in *Proceedings of the 25th CAADRIA Conference*, 2020. doi: https://doi.org/10.52842/conf.caadria.2020.1.385.
- [23] L. Wang, P. Janssen, K. W. Chen, Z. Tong, and G. Ji, "Subtractive Building Massing for Performance-Based Architectural Design Exploration: A Case Study of Daylighting Optimization," *Sustainability*, vol. 11, no. 24, p. 6965, Dec. 2019, doi: 10.3390/su11246965.
- [24] J.-T. Jin and J.-W. Jeong, "Optimization of a free-form building shape to minimize external thermal load using genetic algorithm," *Energy and Buildings*, vol. 85, pp. 473–482, Dec. 2014, doi: 10.1016/j.enbuild.2014.09.080.
- [25]M. Lotteau, P. Loubet, and G. Sonnemann, "An analysis to understand how the shape of a concrete residential building influences its embodied energy and embodied carbon," *Energy and Buildings*, vol. 154, pp. 1–11, Nov. 2017, doi: 10.1016/j.enbuild.2017.08.048.
- [26] C. Preisinger and M. Heimrath, "Karamba—A Toolkit for Parametric Structural Design," *Structural Engineering International*, vol. 24, no. 2, pp. 217–221, May 2014, doi: 10.2749/101686614X13830790993483.
- [27]N. Brown, S. Tseranidis, and C. Mueller, "Multi-objective optimization for diversity and performance in conceptual structural design," presented at the International Association for Shell and Spatial Structures (IASS) Symposium 2015, Amsterdam, 2015.
- [28] J. M. Broyles, J. P. Gevaudan, M. W. Hopper, R. L. Solnosky, and N. C. Brown, "Equations for early-stage design embodied carbon estimation for concrete floors of varying loading and strength," *Engineering Structures*, vol. 301, p. 117369, Feb. 2024, doi: 10.1016/j.engstruct.2023.117369.
- [29]K. Feickert and C. T. Mueller, "Thin shell foundations: Quantification of embodied carbon reduction through materially efficient geometry," *Archit. Struct. Constr.*, Nov. 2023, doi: 10.1007/s44150-023-00101-z.
- [30]D. Fang, D. Fannon, and M. Eckelman, "Bottom-up Estimates of Embodied Carbon in the US Building Stock to Inform Future Directions in Low-Carbon Design and Construction," presented at the Under review, 2025.
- [31] W. Craft, P. Oldfield, G. Reinmuth, D. Hadley, S. Balmforth, and A. Nguyen, "Towards net-zero embodied carbon: Investigating the potential for ambitious embodied carbon reductions in Australian office buildings," *Sustainable Cities and Society*, vol. 113, p. 105702, Oct. 2024, doi: 10.1016/j.scs.2024.105702.
- [32]F. Wong and Y. Tang, "Comparative Embodied Carbon Analysis of the Prefabrication Elements compared with In-situ Elements in Residential Building Development of Hong Kong," *International Journal of Civil and Environmental Engineering*, 2012.
- [33]B. Waldman, A. Hyatt, S. Carlisle, J. Palmeri, and K. Simonen, "2023 Carbon Leadership Forum North American Material Baselines," Carbon Leadership Forum, University of Washington, Seattle, WA, Baseline Report, (version 2), Aug. 2023. [Online]. Available: http://hdl.handle.net/1773/49965
- [34]Dezeen, "Irregularly stacked boxes," Dezeen. [Online]. Available: https://www.dezeen.com/tag/irregularly-stacked-boxes/
- [35] J. Geleff, "Anomalous Volumes: 11 Modular Buildings With Stacked Configurations," Architizer. [Online]. Available: https://architizer.com/blog/inspiration/collections/stacked/

Proceedings of the IASS Annual Symposium 2025 The living past as a source of innovation

- [36] S. Davidson, Grasshopper 3D. (2025). [Online]. Available: https://www.grasshopper3d.com/
- [37]Digital Structures, *Design Space Exploration*. [Online]. Available: https://www.food4rhino.com/en/app/design-space-exploration
- [38] K. Feickert and C. T. Mueller, "Algorithmic investigation of structural system utility for urban development reusing existing foundations," in *IASS Annual Symposium 2023*, Melbourne, Australia, Jul. 2023.
- [39] International Code Council, "2021 International Building Code (IBC)," International Code Council, Inc., 2021.
- [40] Vulcraft, "Vulcraft Steel Deck," Nucor, 2021. [Online]. Available: https://vulcraft.com/products/deck
- [41] N. P. Kurian, *Design of Foundation Systems: Principles and Practices*, 3rd ed. Alpha Science International Ltd., 2004.
- [42] Bureau of Indian Standards, "IS 456: Plain and Reinforced Concrete Code of Practice," 2000.
- [43] American Concrete Institute, "Building Code Requirements for Structural Concrete (ACI 318-19)," ACI Standard, ANSI Standard ACI 318-19, 2022.
- [44]M. Ismail and C. Mueller, "Minimizing embodied energy of reinforced concrete floor systems in developing countries through shape optimization," *Engineering Structures*, vol. 246, p. 112955, Nov. 2021, doi: 10.1016/j.engstruct.2021.112955.
- [45] National Ready Mixed Concrete Association, "Environmental Product Declaration: NRMCA Member Industry-Average EPD for Ready Mixed Concrete." Jan. 03, 2022.
- [46] Concrete Reinforcing Steel Institute, "Environmental Product Declaration: Steel Reinforcement Bar." Sep. 20, 2022.
- [47] American Institute of Steel Construction, "Environmental Product Declaration: Fabricated Hot-Rolled Structural Sections." Jan. 01, 2021.